Train Tracking and Shadowing Estimation Based on Received Signal Strength

Hadi Noureddine[1,2], Damien Castelain[1], and Ramesh Pyndiah[2]

[1] Mitsubishi Electric R&D Centre Europe, France
[2] Telecom Bretagne, France

Abstract. In this work, we present an on-board solution for train position tracking that can be used in cases of GPS failures and that does not suffer from the error accumulation problem of Dead Reckoning (DR). It is based on Received Signal Strength (RSS) measured in radio communication systems by several mobile stations having antennas placed on top of different carriages of the train. As the RSS is affected by the slow fading or shadowing, both the position and the shadowing are jointly tracked. We estimate the shadowing atlas consisting of the shadowing maps along the railway of the different base stations. The proposed solution applies Bayesian filtering for efficiently processing the observations.

Keywords: Train tracking, received signal strength, shadowing, shadowing atlas, spatial correlation, Gaussian process, Bayesian filtering, particle filters.

1 Introduction

Reliable and accurate knowledge of train position and speed plays an important role in avoiding collisions and optimizing the traffic by increasing lines capacities. In classical train control systems, localization is based on track side equipments. The new trends in design of train control systems consist of integrating on-board solutions so as to reduce the need of track-side equipments with their inherent roll-out and maintenance costs and to simplify the deployment of new technologies and configuration changes.

Several methods for on-board position measurements are discussed in [1]. These methods are tachometers, Inertial Navigation Systems (INS) (e.g. accelerometers and gyroscopes), Doppler effect and GPS (and possibly other Global Navigation Satellite Systems such as GALILEO).

The GPS solution provides a good precision when sufficient non-obstructed satellite signals are available. When the GPS fails (e.g. tunnels, valleys, some urban areas), other solutions are required. In [2], dead reckoning the train position from on-board sensors (odometers and accelerometers) is performed during the GPS failures where a data fusion approach based on Kalman filtering is developed. All the above-mentioned technologies but the GPS are DR as the current position is estimated based on a previous position and an estimation of the traveled distance over elapsed time. The performance of DR deteriorates

with time due to error accumulation and a way is needed to compensate this error especially if the GPS failure lasts for a long time duration.

In this paper, we consider the use of RSS measurements in radio communication systems for on-board train positioning. A radio communication system can be either dedicated for communication between the train and the railway regulation control centers (e.g. GSM-R) or a public network offering services to passengers. This solution does not suffer from error accumulation of DR and can be integrated with on-board sensors that can give more information and improve the accuracy.

The RSS measurements are affected by the slow fading or shadowing. The shadowing can be divided into two parts: A time variant part caused by moving obstacles (e.g. a nearby train) and a time invariant one which is function of the position. In the following, we call shadowing the time invariant part. The shadowing in decibels (dB) is modeled by a Gaussian random process along the railway as it is spatially correlated [3] and log-normally distributed [4]. For one base station, we call this process a shadowing map. The shadowing of several base stations is also cross-correlated as reported in [7]. We define the shadowing 'atlas' being the collection of the maps of the different base stations. The knowledge of the shadowing improves the position estimation and is useful for communication purposes (e.g. handover anticipation).

The train position and the shadowing are jointly tracked. For this purpose, we apply Bayesian filtering for efficiently fusing the incoming measurements by recursively updating the posterior probability distributions of the position and the atlas. Due to the non-linearities encountered, sequential Monte Carlo methods known as particle filters [5] will be implemented for approximating the probability density functions.

This paper is organized as follows. In Section 2, the motion model describing the evolution of the train position and the RSS observation model are presented. In Section 3, we introduce the shadowing atlas and show how it can be updated based on RSS measurements when the train position is known. In Section 4, Bayesian filtering and particle filters implementation are presented. Simulation results and conclusions are presented in Sections 5 and 6.

2 System Model

In this section, we describe the motion model of the train and the RSS observation model. They allow for computing the a priori and likelihood probabilities in the Bayesian filtering processing, respectively.

2.1 Motion Model

The train is constrained to move on a known railway track and the position is defined as the Cartesian coordinate of a reference point belonging to the train. The rail can be seen as a parametric curve of one parameter that we call rail coordinate. We assume that the length of the rail (in meters (m)) between two

rail coordinates r_1 and r_2 is equal to the absolute value of $r_1 - r_2$. The train position can be described by the rail coordinate as there is a mapping to the Cartesian coordinates. The train speed is the derivative of the rail coordinate.

At time kT, where $k \in \mathbb{N}$ and T is a time step, we define the state vector $\mathbf{s}_k$ comprising the scalar rail coordinate r_k, the scalar speed v_k and possibly other kinematic parameters (e.g. acceleration).

$\mathbf{s}_k$ is issued from a known Markov process of initial distribution $p(\mathbf{s}_0)$ and transition probability $p(\mathbf{s}_k|\mathbf{s}_{k-1})$.

2.2 RSS Observation Model

We consider several mobile stations having their antennas placed on the top of different carriages of the train for a better sensitivity and penetration losses avoidance. The antennas are spaced enough (several meters to several tens of meters depending on the train size) so that the shadowing values are different at two antennas' positions for the same time instant. We denote N_{MS} the number of these antennas. RSS measurements are made in order to estimate the signal attenuation due to path loss and shadowing. They are usually obtained by low-pass filtering the received power in order to remove the small scale fading. The used filter must be sufficiently narrow in bandwidth to remove the multipath fluctuations, yet sufficiently wide to track the shadow fading.

A simple filtering solution is the sample-average which returns the average of a set of discrete time samples in dB. In [8], simulations in a flat Rayleigh environment with a carrier frequency of $900MHz$ show that a root mean square error of less than $1.6dB$ can be achieved by using the sample-average estimator. This result is obtained by considering a shadowing standard deviation of $\sigma_{sh} = 10dB$ and an exponential correlation function:

$$E\{\epsilon(\mathbf{x_1})\epsilon(\mathbf{x_2})\} = \sigma_{sh} exp(-ln(2)\|\mathbf{x_1} - \mathbf{x_2}\|/d_{corr}) \tag{1}$$

where $\epsilon(\mathbf{x_i})$ is the shadowing at position $\mathbf{x_i}$ and $d_{corr} = 346m$ which is the value estimated in [3] for suburban areas. Under a Rician fading, the error is smaller as the variance of the Rice distribution decreases with the ratio of the specular power to the scattered power. As mentioned in [9], the error can be reduced if the channel bandwidth is sufficiently wide so that several paths can be resolved or if the mobile station has multiple nearby antennas (these antennas are spaced of the order of the wavelength and deliver one RSS measurement as they are affected by the same path loss and shadowing values). The remaining error after filtering is nearly Gaussian distributed.

Fast fading of train radio channels has been investigated in [10] . The measurements showed that only a weak multipath propagation exists and the radio environment is mainly rural. The rural area model is also adopted for tunnels. These studies have also shown that a significant line of sight component exists especially when the base stations are on the track side.

We model the RSS measured by a mobile station having the antenna at position $\mathbf{x}$ as

$$y = f(\mathbf{x}) + \epsilon(\mathbf{x}) + n \tag{2}$$

where f is a deterministic path loss function, ϵ is the shadowing and n is a Gaussian error gathering the time variant shadowing, average power estimation and other non-shadowing errors. Many general path loss prediction models for different deployment environments have been developed. We don't investigate here the path loss model that we assume to be know. In [10], a standard deviation of the shadowing between 1.2 and $3.7dB$ is reported over several railway lines.

3 Shadowing Atlas

3.1 Definition

For one base station, the shadowing is represented by a vector of real values where the rail is discretized and each vector entry corresponds to a discrete position. We call this vector a shadowing map. To obtain the value of the shadowing at an arbitrary position of the rail, we apply a piecewise constant interpolation by assigning the same value of the nearest point having an entry in the shadowing map. In fact, this shadowing map is not perfectly known and can be described by a Gaussian random vector of known mean and covariance. For several base stations, we define the shadowing atlas as being a collection of the shadowing maps obtained by a concatenation of the vectors.

We denote L_{map} the size of the shadowing map vector and $L_{atlas} = N_{BS} \times L_{map}$ the size of the atlas where N_{BS} is the number of base stations encountered along the railway. The size of the atlas covariance matrix is a large $L_{atlas} \times L_{atlas}$ sparse matrix thanks to the low shadowing spatial correlation between distant positions. We can also reduce N_{BS} and L_{map} by considering an atlas for a sector of the railway.

3.2 Atlas Update

Here, we describe how to update the atlas based on RSS measurements made at a known train position.

At time kT, we denote l_k the number of RSS measurements made by the N_{MS} train antennas. The positions of the antennas can be easily deduced from the rail coordinate r_k. The observation vector of size l_k is

$$\begin{aligned} \mathbf{y}_k &= \mathbf{f}_k(r_k) + \mathbf{\Sigma}_k(r_k) + \mathbf{n}_k \\ &= \mathbf{f}_k(r_k) + \mathbf{H}_k\mathbf{\Lambda} + \mathbf{n}_k \end{aligned} \tag{3}$$

where $\mathbf{f}_k(r_k)$ and $\mathbf{\Sigma}_k(r_k)$ are the path loss vector and the shadowing vector respectively, $\mathbf{n}_k$ is the Gaussian error process, $\mathbf{\Lambda}$ is the shadowing atlas vector of size L_{atlas}, and $\mathbf{H}_k$ is an $l_k \times L_{atlas}$ matrix satisfying $\mathbf{H}_k(i, j + L_{map} \times (l-1)) = 1$ if the i^{th} measurement is made with l^{th} base station and the corresponding shadowing has the j^{th} entry in the map vector, and otherwise it is equal to zero.

Denote $\mathbf{M}_{k-1}$ and $\mathbf{C}_{k-1}$ the mean and covariance of $\mathbf{\Lambda}$ at time $(k-1)T$ respectively and assume that the process $\mathbf{n}_k$ is white with respect to time. The observation $\mathbf{y}_k$, which is a linear function of $\mathbf{\Lambda}$, is used to update $\mathbf{M}_k$ and $\mathbf{C}_k$

by means of a linear Minimum Mean Square Error (MMSE) estimator [6] as follows:

$$\mathbf{M}_k = \mathbf{M}_{k-1} + \mathbf{Q}_k(\mathbf{y}_k - \mathbf{f}_k(r_k) - \mathbf{H}_k\mathbf{M}_{k-1}) \tag{4}$$

and

$$\mathbf{C}_k = \mathbf{C}_{k-1} - \mathbf{Q}_k\mathbf{H}_k\mathbf{C}_{k-1} \tag{5}$$

where $\mathbf{Q}_k$ is the gain factor given by:

$$\mathbf{Q}_k = \mathbf{C}_{k-1}\mathbf{H}_k^T(E\{\mathbf{n}_k\mathbf{n}_k^T\} + \mathbf{H}_k\mathbf{C}_{k-1}\mathbf{H}_k^T)^{-1}. \tag{6}$$

In the next section, we describe how to perform this estimation when the position is not perfectly known.

4 Bayesian Tracking Solution

In this section, we present the Bayesian filtering adapted to our tracking problem and its implementation using particle filters.

4.1 Bayesian Filtering

A Bayesian filtering consists of determining recursively in time the posterior distribution $p(\mathbf{s}_{0:k}|\mathbf{y}_{1:k}, \mathbf{u}_{1:k})$, where we denote by $\mathbf{z}_{0:k} = [\mathbf{z}_0^T, \cdots, \mathbf{z}_k^T]^T$ for any sequence $\mathbf{z}_k$, $\mathbf{y}_k$ is the RSS observation vector and $\mathbf{u}_{1:k}$ is an observation vector that might be obtained from INS sensors. The goal is to apply the MMSE estimator:

$$\hat{\mathbf{s}}_k = \int \mathbf{s}_k p(\mathbf{s}_{0:k}|\mathbf{y}_{1:k}, \mathbf{u}_{1:k})\mathrm{d}\mathbf{s}_{0:k}. \tag{7}$$

This posterior distribution allows to compute $p(\mathbf{\Lambda}|\mathbf{y}_{1:k}, \mathbf{u}_{1:k})$ as follows:

$$p(\mathbf{\Lambda}|\mathbf{y}_{1:k}, \mathbf{u}_{1:k}) = \int p(\mathbf{\Lambda}|\mathbf{s}_{0:k}, \mathbf{y}_{1:k})p(\mathbf{s}_{0:k}|\mathbf{y}_{1:k}, \mathbf{u}_{1:k})\mathrm{d}\mathbf{s}_{0:k} \tag{8}$$

where $p(\mathbf{\Lambda}|\mathbf{s}_{0:k}, \mathbf{y}_{1:k})$ is a Gaussian distribution whose parameters can be estimated using the linear MMSE estimator described previously.

The distribution $p(\mathbf{s}_{0:k}|\mathbf{y}_{1:k}, \mathbf{u}_{1:k})$ is computed recursively according to

$$\begin{aligned} &p(\mathbf{s}_{0:k}|\mathbf{y}_{1:k}, \mathbf{u}_{1:k}) \propto \\ &p(\mathbf{s}_{0:k-1}|\mathbf{y}_{1:k-1}, \mathbf{u}_{1:k-1})p(\mathbf{s}_k|\mathbf{s}_{k-1})p(\mathbf{u}_k|\mathbf{s}_{k-1}, \mathbf{s}_k)p(\mathbf{y}_k|\mathbf{s}_{0:k}, \mathbf{y}_{1:k-1}). \end{aligned} \tag{9}$$

By assuming that the error process $\mathbf{n}_k$ is white, the observations at different instants are independent given the atlas:

$$p(\mathbf{y}_i, \mathbf{y}_j|\mathbf{s}_i, \mathbf{s}_j, \mathbf{\Lambda}) = p(\mathbf{y}_i|\mathbf{s}_i, \mathbf{\Lambda})p(\mathbf{y}_j|\mathbf{s}_j, \mathbf{\Lambda}). \tag{10}$$

Thus, a possible computation of $p(\mathbf{y}_k|\mathbf{s}_{0:k}, \mathbf{y}_{1:k-1})$ is

$$p(\mathbf{y}_k|\mathbf{s}_{0:k}, \mathbf{y}_{1:k-1}) = \int p(\mathbf{y}_k|\mathbf{\Lambda}, \mathbf{s}_k)p(\mathbf{\Lambda}|\mathbf{s}_{0:k-1}, \mathbf{y}_{1:k-1})\mathrm{d}\mathbf{\Lambda} \tag{11}$$

Equations (7) and (8) are analytically untraceable since the observation equation (3) is non-linear with respect to r_k and $\mathbf{H}_k$ depends on r_k. A solution based on particle filters [5], which apply sequential Monte Carlo methods for approximating numerically the posterior densities, is presented in the following.

4.2 Implementation Using Particle Filters

Assume that at time $(k-1)T$, $p(\mathbf{s}_{0:k-1}|\mathbf{y}_{1:k-1}, \mathbf{u}_{1:k-1})$ is approximated by the set of M weighted trajectories $\left\{w^i_{k-1}, \mathbf{s}^i_{0:k-1}\right\}_{i=1}^{M}$:

$$p(\mathbf{s}_{0:k-1}|\mathbf{y}_{1:k-1}, \mathbf{u}_{1:k-1}) \cong \sum_i w^i_{k-1}\delta(\mathbf{s}_{0:k-1}, \mathbf{s}^i_{0:k-1}) \tag{12}$$

where δ is the Kronecker delta function.

The atlas posterior distribution is computed according to (8):

$$p(\mathbf{\Lambda}|\mathbf{y}_{1:k-1}, \mathbf{u}_{1:k-1}) \cong \sum_i w^i_{k-1} p(\mathbf{\Lambda}|\mathbf{s}^i_{0:k-1}, \mathbf{y}_{1:k-1}). \tag{13}$$

The Gaussian distributions $p(\mathbf{\Lambda}|\mathbf{s}^i_{0:k-1}, \mathbf{y}_{1:k-1}) = N(\mathbf{M}^i_{k-1}, \mathbf{C}^i_{k-1})$ are obtained using the linear MMSE estimator by one of two methods: The first method is to update $p(\mathbf{\Lambda}|\mathbf{s}^i_{0:k-2}, \mathbf{y}_{1:k-2})$ at each time step where a huge amount of memory is needed in order to store the M atlases. The second method is to compute it from scratch at each time step using all the previous observations but with a complexity that increases with time.

We propose a suboptimal solution that approximates the weighted mixture of Gaussian distributions $\left\{w^i_{k-1}, N(\mathbf{M}^i_{k-1}, \mathbf{C}^i_{k-1})\right\}_{i=1}^{M}$ by a single Gaussian one $N(\hat{\mathbf{M}}_{k-1}, \hat{\mathbf{C}}_{k-1})$. This operation is repeated every q time steps by substituting $p(\mathbf{\Lambda}|\mathbf{s}^i_{0:k+q-1}, \mathbf{y}_{1:k+q-1})$ by $p(\mathbf{\Lambda}|\mathbf{s}^i_{k:k+q-1}, \mathbf{y}_{k:k+q-1})$ where the initial distribution $p(\mathbf{\Lambda})$ is substituted by $N(\hat{\mathbf{M}}_{k-1}, \hat{\mathbf{C}}_{k-1})$.

The posterior distribution $p(\mathbf{s}_{0:k}|\mathbf{y}_{1:k}, \mathbf{u}_{1:k})$ at time kT can be obtained in three steps that are summarized in Fig. 1.

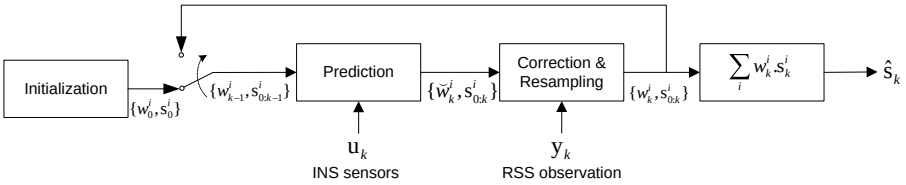

Fig. 1. Particle filter for estimating the state vector $\mathbf{s}_k$.

Prediction Step The predictive distribution $p(\mathbf{s}_{0:k}|\mathbf{y}_{1:k-1}, \mathbf{u}_{1:k})$ can be written as

$$\begin{aligned} p(\mathbf{s}_{0:k}|\mathbf{y}_{1:k-1}, \mathbf{u}_{1:k}) &\cong \textit{constant} \times \sum_i w^i_{k-1} p(\mathbf{u}_k|\mathbf{s}^i_{k-1}) p(\mathbf{s}_k|\mathbf{s}^i_{k-1}, \mathbf{u}_k)\delta(\mathbf{s}_{0:k-1}, \mathbf{s}^i_{0:k-1}) \\ &\cong \sum_i \breve{w}^i_k p(\mathbf{s}_k|\mathbf{s}^i_{k-1}, \mathbf{u}_k)\delta(\mathbf{s}_{0:k-1}, \mathbf{s}^i_{0:k-1}) \end{aligned} \tag{14}$$

where $\breve{w}_k^i \propto w_{k-1}^i p(\mathbf{u}_k|\mathbf{s}_{k-1}^i)$. A Monte Carlo approximation of this distribution is obtained by drawing $\mathbf{s}_k^i$ from $p(\mathbf{s}_k|\mathbf{s}_{k-1}^i, \mathbf{u}_k)$:

$$p(\mathbf{s}_{0:k}|\mathbf{y}_{1:k-1}, \mathbf{u}_{1:k}) \cong \sum_i \breve{w}_k^i \delta(\mathbf{s}_{0:k}, \mathbf{s}_{0:k}^i). \tag{15}$$

The measurement $\mathbf{u}_k$ is included in this step since the INS observation models are in general linear with respect to the state and samples can be easily drawn from $p(\mathbf{s}_k|\mathbf{s}_{k-1}^i, \mathbf{u}_k)$.

Correction Step In this step, the observation $\mathbf{y}_k$ is used in order to compute $p(\mathbf{s}_{0:k}|\mathbf{y}_{1:k}, \mathbf{u}_{1:k})$ by updating the weights according to

$$w_k^i \propto \breve{w}_k^i p(\mathbf{y}_k|\mathbf{s}_{0:k}^i, \mathbf{y}_{1:k-1}). \tag{16}$$

The value $p(\mathbf{y}_k|\mathbf{s}_{0:k}^i, \mathbf{y}_{1:k-1})$ can be estimated with two methods:

- Using (11) with the complexity or memory drawbacks mentioned above.
- Using the following equation:

$$\begin{aligned} &p(\mathbf{y}_k|\mathbf{s}_{0:k}^i, \mathbf{y}_{1:k-1}) = \\ &\int p(\mathbf{y}_k|\mathbf{\Sigma}_k, \mathbf{s}_k^i) p(\mathbf{\Sigma}_k|\mathbf{\Sigma}_{0:k-1}, \mathbf{s}_{0:k}^i) p(\mathbf{\Sigma}_{0:k-1}|\mathbf{s}_{0:k-1}^i \mathbf{y}_{1:k-1}) \mathrm{d}\mathbf{\Sigma}_{0:k} \end{aligned} \tag{17}$$

  where $\mathbf{\Sigma}_{0:k-1} = [\mathbf{\Sigma}_0^T, \cdots, \mathbf{\Sigma}_{k-1}^T]^T$ and $\mathbf{\Sigma}_k = \mathbf{\Sigma}_k(\mathbf{r}_k)$.
  The distribution $p(\mathbf{\Sigma}_k|\mathbf{\Sigma}_{0:k-1}, \mathbf{s}_{0:k}^i)$ can be computed from the initial a priori atlas distribution $p(\mathbf{\Lambda})$, and $p(\mathbf{\Sigma}_{0:k-1}|\mathbf{s}_{0:k-1}^i \mathbf{y}_{1:k-1})$ is obtained by a Kalman filter. As the trains run on nearly straight rails, the shadowing at a given time step is uncorrelated with the shadowing at much older time steps and the process $p(\mathbf{\Sigma}_k|\mathbf{\Sigma}_{0:k-1}, \mathbf{s}_{0:k}^i)$ can be replaced by a p-order process $p(\mathbf{\Sigma}_k|\mathbf{\Sigma}_{k-p:k-1}, \mathbf{s}_{k-p:k}^i)$ and thus limiting the complexity.

Resampling Step In order to avoid the weights degeneracy due to the increase of the variance of the set $\{w_k^i\}_{i=1}^M$ [5], a resampling step is performed. Thus, some trajectories of weak weights are eliminated and some of strong weights repeated. We execute this step when the effective number of particles $N_{eff} = 1/\sum_i (w_k^i)^2$ falls below a threshold.

5 Simulation results

In this section we introduce the motion and the observation model scenarios assumed for the computer simulations and show the results.

The motion of the train is modeled by a simple linear Markov process. The state vector is $\mathbf{s}_k = [r_k, v_k]^T$ where r_k is the rail coordinate and v_k is the speed. The state vector $\mathbf{s}_k$ evolves according to the following difference equation:

$$\mathbf{s}_k = \begin{bmatrix} 1 & T \\ 0 & 1 \end{bmatrix} \mathbf{s}_{k-1} + \begin{bmatrix} 0 \\ T \end{bmatrix} (a_{k-1} + e_{k-1}) \tag{18}$$

where a_{k-1} is the acceleration vector provided by an accelerometer and e_{k-1} is a Gaussian variable that accounts for the acceleration estimation errors. We take the standard deviation of e_{k-1} equal to $1m/s^2$ and the mean equal to zero (the accelerometer bias is assumed to be known, otherwise it can be added to the state vector and tracked by the particle filter). The time step is $T = 0.5s$. The train moves on a linear rail of length $4km$ and there are two base stations located at $[-1390, -1032]^T$ and $[1589, -688]^T$ (in meters) as shown in Fig. 2. The train is moving from the left to the right. The speed is linearly increasing

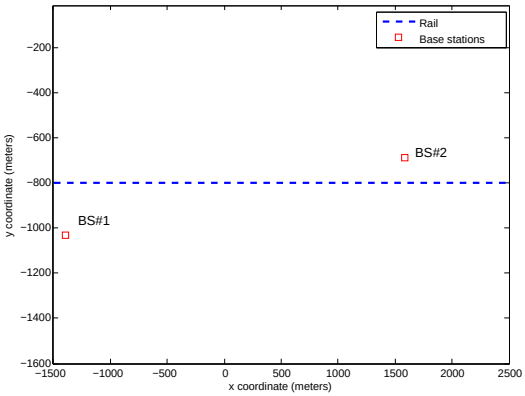

Fig. 2. Rail and base stations deployment.

with time from $200km/h$ to $250km/h$. The train takes $64s$ to make the $4km$.

The shadowing has a standard deviation equal to $\sigma_{sh} = 4dB$ and is correlated according to the exponential function (1) and we set $d_{corr} = 200m$. The cross-correlation coefficient from two different base stations is constant and equal to 0.5, for simplicity. The initial atlas mean is equal to zero and the atlas covariance matrix is constructed according these parameters values.

The measurement error $\mathbf{n}_k$ is a zeros mean white Gaussian process with a diagonal covariance matrix and diagonal entries equal to $4dB^2$. In fact, to have a white process, the error remaining after averaging out the fast fading has to be white, and this can be obtained by a displacement of the antennas of about $\lambda/2$ perpendicular to the motion direction, as shown in Fig. 3.

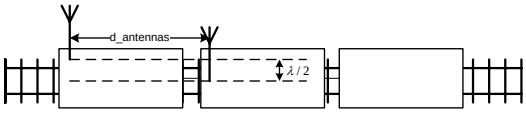

Fig. 3. Train antennas with a displacement of $\lambda/2$.

For the path loss, we consider the Macro-cell system simulation model defined in [11] with omnidirectional base station antennas.

For the particle filter implementation, we take $M = 100$ particles. This number is sufficient since the dimension of the state vector is low (equal to two). We also replace the Gaussian process $p(\mathbf{\Sigma}_k|\mathbf{\Sigma}_{0:k-1}, \mathbf{s}^i_{0:k})$ in (17) by a first-order process $p(\mathbf{\Sigma}_k|\mathbf{\Sigma}_{k-1}, \mathbf{s}^i_{k-1:k})$. At low train speeds, it might be useful to consider higher orders of this process as the antennas at two non-consecutive time steps can be overlapping as shown in Fig. 4(b).

In Fig. 5, we plot the Root Mean Square Error (RMSE) of the position. The RMSE of the DR solution based on the accelerometer observations is increasing with time. The initial position and speed are perfectly known.

The antennas placed on the train are equidistant. We can see that with 4 antennas, the performance is better when the distance between two consecutive antennas is $20m$ (d_anntennas in Fig. 3). A possible justification of this result is that the antennas are overlapping at two consecutive time steps when the separation is equal to $20m$ leading to a better estimation of the shadowing, while this overlap does not occur for a separation of $10m$ as shown in Fig. 4. Moreover, the shadowing values affecting the different antennas measurements are less correlated for larger separations, and thus, leading to a higher diversity. We remark that the RMSE begins to decrease after about $40s$ as the train approaches $BS\#2$ since the path loss decreases logarithmitically with the distance which is better estimated near a base station

In Fig. 6, the RMSE of the shadowing map of $BS\#1$ is plotted after one passing of the train. Later on, the obtained atlas distribution can be used as an initial distribution for other trains passing through the same railway.

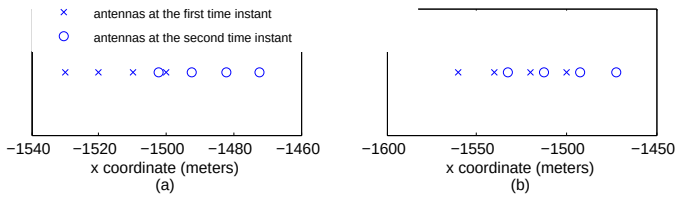

Fig. 4. Antennas positions at two consecutive time instants with separations of (a) $10m$ and (b) $20m$. The velocity is 200 km/h.

6 Conclusions

We presented an on-board solution for train tracking based on the RSS measurements in a radio communication system. It can be integrated with INS sensors and can serve as a long time substitute of the GPS as it does not suffer from error accumulation of DR solutions. We also perform a joint estimation of the shadowing and construct the shadowing atlas.

The atlas estimation can be processed either on-line or off-line where the measurements made during the train travel are saved and processed by a server at the railway station. The initial distribution of the atlas can be downloaded at the railway station. An operation similar to the fingerprinting can be also performed by making RSS measurements at known positions and updating the atlas accordingly.

References

1. Mirabadi, A., Mort, N., Schmid, F.: Application of sensor fusion to railway systems. Multisensor Fusion and Integration for Intelligent Systems, 1996. IEEE/SICE/RSJ International Conference on , vol., no., pp.185-192, 8-11 Dec 1996.
2. Ernest, P., Mazl, R., Preucil, L.: Train locator using inertial sensors and odometer. Intelligent Vehicles Symposium, 2004 IEEE , vol., no., pp. 860- 865, 14-17 June 2004.
3. Gudmundson, M.: Correlation model for shadow fading in mobile radio systems. Electronics Letters , vol.27, no.23, pp.2145-2146, 7 Nov. 1991.
4. Rappaport, T.: Wireless Communications: Principles and Practice. Prentice Hall PTR, Upper Saddle River, NJ, USA, 2001.
5. Doucet, A.: On sequential simulation-based methods for bayesian filtering. Technical report, 1998.
6. Kay, Steven M.: Fundamentals of Statistical Signal Processing, Vol I: Estimation Theory (v. 1). Prentice Hall, 1 edition, April 1993.
7. Sorensen, T.B.: Slow fading cross-correlation against azimuth separation of base stations. Electronics Letters , vol.35, no.2, pp.127-129, 21 Jan 1999.
8. Tao Jiang, Sidiropoulos, N.D., Giannakis, G.B.: Kalman filtering for power estimation in mobile communications. Wireless Communications, IEEE Transactions on , vol.2, no.1, pp. 151- 161, Jan. 2003.
9. Goldsmith, A.J., Greenstein, L.J., Foschini, G.J.: Error statistics of real-time power measurements in cellular channels with multipath and shadowing. Vehicular Technology, IEEE Transactions on , vol.43, no.3, pp.439-446, Aug 1994.
10. Goller, M.: Application of GSM in high speed trains: measurements and simulations. Radiocommunications in Transportation, IEE Colloquium on , vol., no., pp.5/1-5/7, 16 May 1995.
11. 3GPP. Tr 25.814, physical layer aspects for evolved universal terrestrial radio access (utra) (release 7). September 2006.

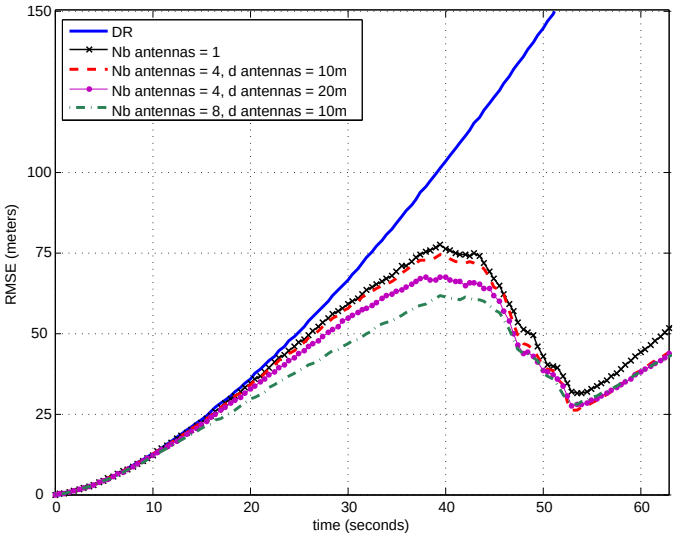

Fig. 5. RMSE of the train position.

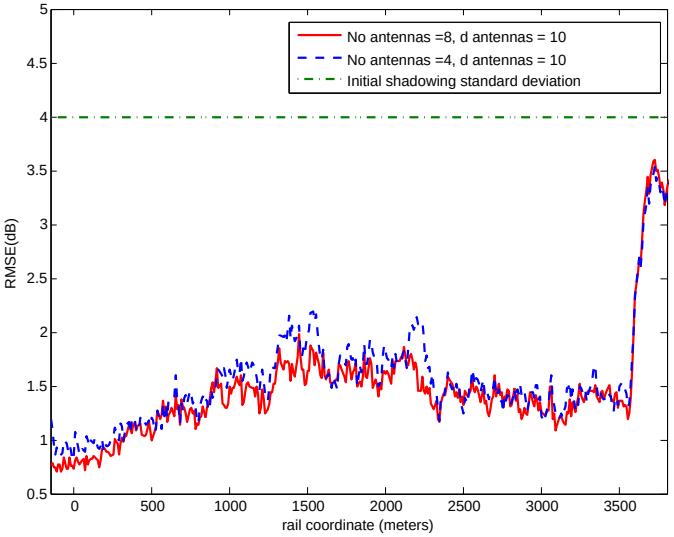

Fig. 6. RMSE of the Shadowing map estimation of BS#1.